Dilaton black holes with power law electrodynamics

M. Dehghani* and M. R. Setare†

Department of Physics, Razi University, P.O. Box 6741414971, Kermanshah, Iran

(Received 14 November 2018; published 12 August 2019)

Here we obtain the new four-dimensional black hole solutions to the Einstein-power-Maxwell-dilaton gravity theory. We solve the coupled scalar, electromagnetic, and gravitational field equations in a static and spherically symmetric geometry and show that dilatonic potential, as the solution to the scalar field equation, can be written as a generalized Liouville potential. We obtain three classes of novel charged dilaton black hole solutions, in the presence of power law nonlinear electrodynamics, which are asymptotically nonflat and non-anti-de Sitter. Then we calculate the conserved and thermodynamic quantities from geometrical and thermodynamical approaches, separately. Since the results of these two alternative approaches are identical, one can argue that the first law of black hole thermodynamics is valid for all of the new black hole solutions. We study thermodynamic stability or phase transition of the black holes using the canonical ensemble method. The points of type-1 and type-2 phase transitions and the ranges at which the black holes remain stable are indicated by considering the heat capacity of the black hole solutions. The global stability of the black holes is studied through the grand canonical ensemble method. Regarding the Gibbs free energy of the black holes, we find the points of Hawking-Page phase transition and ranges of the horizon radii at which the black holes are globally stable.

DOI: 10.1103/PhysRevD.100.044022

I. INTRODUCTION

It seems that, at least at the high-energy regime, Einstein's action alone is not sufficient to give to describe the Universe completely. This action has been modified by the superstring terms which are scalar tensor in nature. The low-energy limit of the string theory leads to the Einstein gravity coupled to a scalar dilaton field [1,2]. Since ever the new string black hole solutions have been found, there has been strong interest in studying the exact solutions to the scalar coupled general relativity known as the Einstein-dilaton gravity theory. In the presence of dilaton field, the asymptotic behavior of the solutions is changed to be neither flat nor anti-de Sitter [(A)dS] [3,4]. Although, existence of the dilatonic black holes in the space-times with negative cosmological constant circumvents the no-hair conjecture, which originally stated that a black hole should be characterized only by its mass, angular momentum, and electric charge [5,6], it has been shown by many authors that Einstein's gravity theory with a coupled scalar field admits exact hairy black hole solutions in three-, four-, and higher-dimensional space-times [7–10].

The studies on the black holes, as the thermodynamic systems, date back to the most outstanding achievements of Hawking and Bekenstein in the context of geometrical physics. According to the laws of black hole thermodynamics, the black hole temperature and entropy are related to the geometrical quantities such as black hole horizon area and surface gravity, respectively. Also, the black hole entropy and temperature together with the black hole mass (energy) satisfy the first law of black hole thermodynamics [11–17].

Besides, thermodynamic stability or phase transition of the black holes is the other important issue that has attracted a lot of attention in recent years. There are alternative approaches for analyzing the thermal stability or thermodynamic phase transition of the black holes. Geometrical thermodynamics is an interesting way for investigation of black hole phase transition. In this method, divergence points of thermodynamical Ricci scalar provide some information related to thermodynamic phase transition points (see [18] and references therein). Making use of the grand canonical ensemble method and noting the signature of the determinant of the Hessian metrics one can find some information about the thermodynamic stability of the physical black holes [9,19,20]. Also, the canonical ensemble method is an interesting way for studying the black hole stability which is based on the behavior of the black hole heat capacity. It is argued that roots and divergence points of the black hole heat capacity represent the two types of phase transitions. In addition, the signature of black hole heat capacity with the black hole charge as a constant enables one to study the thermal stability of the black holes [21–23]. In this paper, we want

*m.dehghani@razi.ac.ir
†rezakord@ipm.ir

to study thermal stability and phase transition in the context of canonical ensemble method as the more fundamental theory.

Recent studies on the thermodynamics of black holes have shown that there is a correspondence between the gravitating fields in anti-de Sitter (AdS) space-time and conformal field theory (CFT) living on the boundary of the AdS space-time. Thus, the thermodynamic properties of black holes in AdS spaces can be identified based on the AdS/CFT correspondence in the high temperature limit [24–26].

Appearance of the infinite electric field and self-energy for the pointlike charged particles, as the famous challenge of Maxwell's theory of classical electrodynamics, was the initial motivation for introducing the various models of nonlinear electrodynamics. The first model of nonlinear electrodynamics, which restricts the electric field of a point charge to an upper bound, was proposed by Born and Infeld in 1935 [27,28]. It was shown that Born-Infeld nonlinear electrodynamics is not the only modification of the linear Maxwell field which keeps the electric field of a charged point particle finite at the origin, other types of nonlinear Lagrangian such as exponential and logarithmic nonlinear electrodynamics can play the same role [29–32]. Nowadays, the theory of nonlinear electrodynamics has got a lot of attention and has provided an interesting research area in the context of geometrical physics and specially in the study of static and rotational black holes. Utilizing the Born-Infeld and the other types of nonlinear electrodynamics, such as logarithmic, exponential, and power law electrodynamics, lead essentially to some new black hole solutions with the physical and thermodynamical properties affected by the model of electrodynamics under consideration [22,23] and [30–35]. In the four-dimensional space-times, the Lagrangian of Maxwell's theory remains invariant under conformal transformations in the form of $g_{\alpha\beta} \to \Omega^2 g_{\alpha\beta}$. Breaking down of the conformal symmetry in the space-times with the dimensions other than four is the other challenge of Maxwell's theory of electrodynamics. Power law theory of nonlinear electrodynamics is the only model of electrodynamics which preserves its conformally invariant property in the space-times with arbitrary dimensions. It has been shown that the Lagrangian of power law nonlinear electrodynamics is invariant under the conformal transformations in the three- four- and higher-dimensional space-times provided that the power is chosen equal to one-fourth of the space-time dimensions [9,36,37]. Since the action of Einstein-dilaton gravity theory is related to that of scalar-tensor gravity theory via conformal transformations, this conformal symmetry of the power law nonlinear electrodynamics makes it more interesting to be considered in the context of geometrical physics and specially in the framework of Einstein-dilaton gravity theory [38–41].

Our mail aim in this paper is to obtain the new exact black hole solutions to the Einstein-power-Maxwell-dilaton gravity theory and to investigate the physical and thermodynamical properties of the solutions. Also, to check the validity of the thermodynamical first law and to perform a thermal stability or phase transition analysis for the new black hole solutions. Indeed, this work can be regarded as the extension of my previous one presented in Ref. [42], named as the Einstein-Maxwell-dilaton gravity theory, to the case of nonlinear electrodynamics by considering the power law Maxwell field.

Our paper is organized as follows. In Sec. II, we obtain equation of motions from four-dimensional Einstein dilatonic action coupled to the power law nonlinear electrodynamics. Then we solve the equations of the scalar, electromagnetic, and tensor fields in a static spherically symmetric geometry and show that the dilatonic potential can be written as the linear combination of Liouville-type potentials. Also, three classes of new black hole solutions of the Einstein-power-Maxwell-dilaton gravity theory have been constructed out, which are asymptotically nonflat and non-AdS. In Sec. III, we study the thermodynamic properties of the novel charged black hole solutions. We obtain the total charge and mass of black hole, as well as the entropy and temperature associated with the black hole horizon. Then we calculate the electric potential of the black holes, relative to a reference point located at infinity relative to the horizon. Moreover, using a Smarr-type mass formula, we obtain the black hole mass as a function of the extensive parameters, charge, and entropy. Using thermodynamical methods, we calculate intensive parameters, temperature, and electric potential, conjugate to the extensive parameters. Compatibility of the results of geometrical and thermodynamical approaches confirms the validity of the first law of black hole thermodynamics, for all classes of the new black hole solutions. In Sec. IV, we investigate the local stability or phase transition of the black holes. By considering the canonical ensemble approach and regarding the black hole heat capacity, with the black hole charge as a constant, a black hole stability analysis has been performed and the points of type-1 and type-2 phase transitions as well as the ranges at which the black holes are locally stable have been determined, precisely. A black hole global stability analysis has been presented in Sec. V. Through the calculation of the black hole Gibbs free energy, the points of the Hawking-Page phase transition and the ranges at which our black holes are globally stable have been characterized. Section VI is devoted to conclusions and discussions.

II. THE FIELD EQUATIONS AND THE BLACK HOLE SOLUTIONS

We consider the following action for the four-dimensional charged black holes in the Einstein gravity theory coupled to a dilatonic potential [42,43]:

$$I = \frac{1}{16\pi}\int \sqrt{-g}d^4x[\mathcal{R} - V(\phi) - 2g^{\mu\nu}\nabla_\mu\phi\nabla_\nu\phi + \mathcal{L}(\mathcal{F},\phi)]. \tag{2.1}$$

Here, $\mathcal{R}$ is the Ricci scalar. ϕ is the scalar field coupled to itself via the potential term $V(\phi)$. The last term is the coupled scalar-electrodynamic Lagrangian. Using the power law nonlinear electrodynamics and in terms of the scalar-electromagnetic coupling constant α, we have [22,23,44]

$$\mathcal{L}(\mathcal{F},\phi) = (-\mathcal{F}e^{-2\alpha\phi})^p, \tag{2.2}$$

where, $\mathcal{F} = F^{\mu\nu}F_{\mu\nu}$ being the Maxwell invariant. In terms of the electromagnetic potential, A_μ, $F_{\mu\nu}$ is defined as $F_{\mu\nu} = \partial_\mu A_\nu - \partial_\nu A_\mu$ and power p is known as the nonlinearity parameter. One expect that in the case $p = 1$, the results of this theory reduce to the Einstein-Maxwell-dilaton gravity theory. By varying the action (2.1), we find the field equations as follows:

$$2\mathcal{R}_{\mu\nu} = V(\phi)g_{\mu\nu} + 4\nabla_\mu\phi\nabla_\nu\phi + \left[(2p-1)g_{\mu\nu} + \frac{2p}{\mathcal{F}}F_{\mu\alpha}F^\alpha_\nu\right]\mathcal{L}(\mathcal{F},\phi), \tag{2.3}$$

$$\nabla_\mu[\mathcal{L}_\mathcal{F}(\mathcal{F},\phi)F^{\mu\nu}] = 0, \qquad \mathcal{L}_\mathcal{F}(\mathcal{F},\phi) \equiv \frac{\partial}{\partial\mathcal{F}}\mathcal{L}(\mathcal{F},\phi), \tag{2.4}$$

$$4\Box\phi = \frac{dV(\phi)}{d\phi} + 2\alpha p\mathcal{L}(\mathcal{F},\phi), \qquad \phi = \phi(r), \tag{2.5}$$

for the gravitational, electromagnetic, and scalar field equations, respectively.

Our ansatz for the four-dimensional spherically symmetric solution to the gravitational field equations is as

$$ds^2 = -W(r)dt^2 + \frac{1}{W(r)}dr^2 + r^2R^2(r)(d\theta^2 + \sin^2\theta d\varphi^2). \tag{2.6}$$

Here, $W(r)$ and $R(r)$ are two unknown functions of r to be determined.

Noting the fact that the only nonzero component of the electromagnetic field is F_{tr} and assuming as a function of r, we have $\mathcal{F} = -2(F_{tr}(r))^2 = -2(-\partial_r A_t(r))^2$. Making use of (2.6) in (2.3), we arrived at the following explicit form of the gravitational equations:

$$rR(r)W''(r) + 2[R(r) + rR'(r)]W'(r) + rR(r)([V(\phi) - \mathcal{L}(\mathcal{F},\phi))] = 0, \tag{2.7}$$

$$rR(r)W''(r) + 2[R(r) + rR'(r)]W'(r) + 4[rR''(r) + 2R'(r) + rR(r)\phi'^2(r)]W(r) + rR(r)[V(\phi) - \mathcal{L}(\mathcal{F},\phi)] = 0, \tag{2.8}$$

$$2rR(r)[R(r) - rR'(r)]W'(r) + 2[(R(r))^2 + r^2R''(r)R(r) + 4rR'(r)R(r) + r^2(R'(r))^2]W(r) + r^2R^2(r)[V(\phi) + (2p-1)\mathcal{L}(\mathcal{F},\phi)] - 2 = 0, \tag{2.9}$$

for tt, rr, and $\theta\theta(\varphi\varphi)$ components, respectively. In overall the paper, prime means derivative with respect to the argument. Subtracting Eq. (2.7) from Eq. (2.8) results in

$$rR''(r) + 2R'(r) + rR(r)\phi'^2(r) = 0. \tag{2.10}$$

The differential equation (2.10) can be written in the following form:

$$\frac{2}{r}\frac{d}{dr}\ln R(r) + \frac{d^2}{dr^2}\ln R(r) + \left(\frac{d}{dr}\ln R(r)\right)^2 + \phi'^2(r) = 0. \tag{2.11}$$

From Eq. (2.11), one can argue that $R(r)$ must be an exponential function of $\phi(r)$. So, we can write $R(r) = e^{\beta\phi(r)}$ in Eq. (2.11), where $\phi = \phi(r)$ satisfies the following equation:

$$\beta\phi'' + (1+\beta^2)\phi'^2 + \frac{2\beta}{r}\phi' = 0. \tag{2.12}$$

The solution of Eq. (2.12), in terms of a positive constant b, can be written as

$$\phi(r) = \gamma\ln\left(\frac{b}{r}\right), \quad \text{with} \quad \gamma = \beta(1+\beta^2)^{-1}. \tag{2.13}$$

We would like to study the effects of the exponential solution (i.e., $R(r) = e^{\beta\phi(r)}$) with both $\beta = \alpha$ and $\beta \neq \alpha$ cases on the thermodynamics behavior of the four-dimensional nonlinearly charged dilatonic black hole solutions. The cases of $\beta = \alpha$ and $\beta \neq \alpha$, with Maxwell's electromagnetic theory, have been studied in Refs. [7,42,45]. Now we want to extend this idea to the charged black hole solutions in the presence of power law nonlinear electrodynamics. For this aim, we solve the field equations, making use of the scalar fields given by Eq. (2.13).

Regarding these solutions together with Eq. (2.6), the solution to the electromagnetic field equation (2.4) is given by following equations:

$$\begin{cases} A_t(r) = \frac{q}{B-1}r^{1-B}, \\ F_{tr}(r) = qr^{-B}, \end{cases} \tag{2.14}$$

where $B = \frac{2}{2p-1}[1 + \gamma(\alpha p - \beta)]$ with $p \neq \frac{1}{2}$ and q is an integration constant related to the total electric charge of the black hole. It will be calculated in the following section. A notable point is that in order to the potential function $A_t(r)$ be physically reasonable (i.e., zero at infinity), the condition $B > 1$ must be fulfilled. In the absence of dilaton field (i.e., $\beta = 0 = \gamma$), this condition reduces as $\frac{2p-3}{2p-1} < 0$ or equivalently $\frac{1}{2} < p < \frac{3}{2}$, which is just the condition encountered in Refs. [23,46].

Now, Eq. (2.9) can be rewritten as

$$W'(r) - \frac{1-2\beta\gamma}{r} W(r) + \frac{r}{2(1-\beta\gamma)} \left[\frac{2}{r^2 R^2(r)} - V(\phi) - (2p-1)\mathcal{L}(\mathcal{F}, \phi) \right] = 0. \tag{2.15}$$

In order to obtain $W(r)$, we should find potential $V(\phi(r))$ as a function of the radial coordinate. For this purpose, we return to the scalar field equation (2.5). It can be written as

$$\frac{dV(\phi)}{d\phi} + \frac{4\gamma}{r} \left(W'(r) - \frac{1-2\beta\gamma}{r} W(r) \right) + 2\alpha p \mathcal{L}(\mathcal{F}, \phi) = 0. \tag{2.16}$$

Combination of the coupled differential equations (2.15) and (2.16) leads to the following first order differential equation:

$$\frac{dV(\phi)}{d\phi} - 2\beta V(\phi) + 2[\alpha p - \beta(2p-1)]\mathcal{L}(\mathcal{F}, \phi) + \frac{4\beta}{r^2 R^2(r)} = 0. \tag{2.17}$$

The solution to the differential (2.17) can be written as the generalized form of the Liouville scalar potential. That is

$$V(\phi) = \begin{cases} 2(\Lambda + \lambda_1)e^{2\phi} + 2\lambda_2 \phi e^{2\phi} + 2\lambda_3 e^{2\beta_0 \phi}, & \text{for } \beta = 1, \\ 2\Lambda e^{2\beta\phi} + 2\Lambda_1 e^{2\beta_1 \phi} + 2\Lambda_2 e^{2\beta_2 \phi}, & \text{for } \beta \neq 1, \end{cases} \tag{2.18}$$

where

$$\beta_0 = p(2B_1 - \alpha), \qquad \lambda_1 = \frac{p(\alpha-2)+1}{B_1 b^{2pB_1}} q^{2p} 2^{p-1},$$
$$\lambda_2 = -\frac{2}{b^2}, \qquad \lambda_3 = -\lambda_1, \qquad B_1 = \frac{1+\alpha p}{2p-1}, \tag{2.19}$$

$$\beta_1 = \frac{1}{\beta}, \qquad \beta_2 = p\left(\frac{B}{\gamma} - \alpha\right), \qquad \Lambda_1 = \frac{\beta^2}{b^2(\beta^2-1)},$$
$$\Lambda_2 = \frac{2^{p-1}\gamma[\alpha p - \beta(2p-1)]q^{2p}}{b^{2pB}[\gamma(\alpha p + \beta) - pB]}. \tag{2.20}$$

It is notable that the solution given by Eq. (2.18) is compatible with the solution obtained in my previous work [42]. We should note that in the absence of dilatonic field ϕ, we have $V(\phi = 0) = 2\Lambda = -6\ell^{-2}$ and the action (2.1) reduces to that of Einstein-Λ-Maxwell theory [47,48].

Now, using Eqs. (2.14), (2.15), and (2.18), the metric function $W(r)$ can be obtained as

$$W(r) = \begin{cases} -\frac{m}{r^{1-2\beta\gamma}} + (1+\beta^2)\left[\frac{1}{1-\beta^2}\left(\frac{r}{b}\right)^{2\beta\gamma} - \frac{\Lambda b^2(1+\beta^2)}{3-\beta^2}\left(\frac{r}{b}\right)^{\frac{2\gamma}{\beta}} + \frac{q^{2p}2^{p-1}\Upsilon(\beta)}{(B-1)b^{2(pB-1)}}\left(\frac{b}{r}\right)^{2\eta}\right], & \text{for } \beta \neq 1, \sqrt{3}, \\ -mr^{1/2} - 2\left[\left(\frac{r}{b}\right)^{2/3} + 2\Lambda(b^3 r)^{\frac{1}{2}}\ln\left(\frac{r}{L}\right) - \frac{2^p q^{2p}\Upsilon(\beta=\sqrt{3})}{(\mathcal{B}-1)b^{2(p\mathcal{B}-1)}}\left(\frac{b}{r}\right)^{2\xi}\right], & \text{for } \beta = \sqrt{3}, \\ -m + 2\left[2 - b^2(\Lambda+\lambda_1) + \ln\left(\frac{b}{r}\right)\right]\left(\frac{r}{b}\right) + \frac{p2^{p+1}q^{2p}}{B_1(B_1-1)b^{2(pB_1-1)}}\left(\frac{b}{r}\right)^{B_1-1}, & \text{for } \beta = 1, \end{cases} \tag{2.21}$$

where m is an integration constant, L is a dimensional constant, and

$$\mathcal{B} = \frac{1+\sqrt{3}\alpha p}{2(2p-1)}, \quad \eta = pB - p\alpha\gamma - 1, \quad \xi = p\left(\mathcal{B} - \frac{\alpha\sqrt{3}}{4}\right) - 1, \quad \Upsilon(\beta) = 2p - 1 - \frac{\beta[\alpha p - \beta(2p-1)]}{p(B-\alpha\gamma)(1+\beta^2) - \beta^2}. \tag{2.22}$$

In the case $p = 1$, the metric function (2.21) is compatible with that of Ref. [42]. The plots of metric functions $W(r)$, presented in Eq. (2.21), have been shown in Figs. 1–3 for $\beta = \alpha$ and $\beta \neq \alpha$ cases, separately. From the curves of Figs. 1–3, it is understood that, for the suitably fixed parameters, the metric functions $W(r)$ can produce black holes with two horizons, extreme black holes and naked singularity black holes for all of $\beta \neq 1, \sqrt{3}$, $\beta = \sqrt{3}$, and $\beta = 1$ cases.

In order to investigate the space time singularities, one needs to calculate the curvature scalars. The Ricci and Kretschmann scalars, after some algebraic calculations, can be written in the following forms:

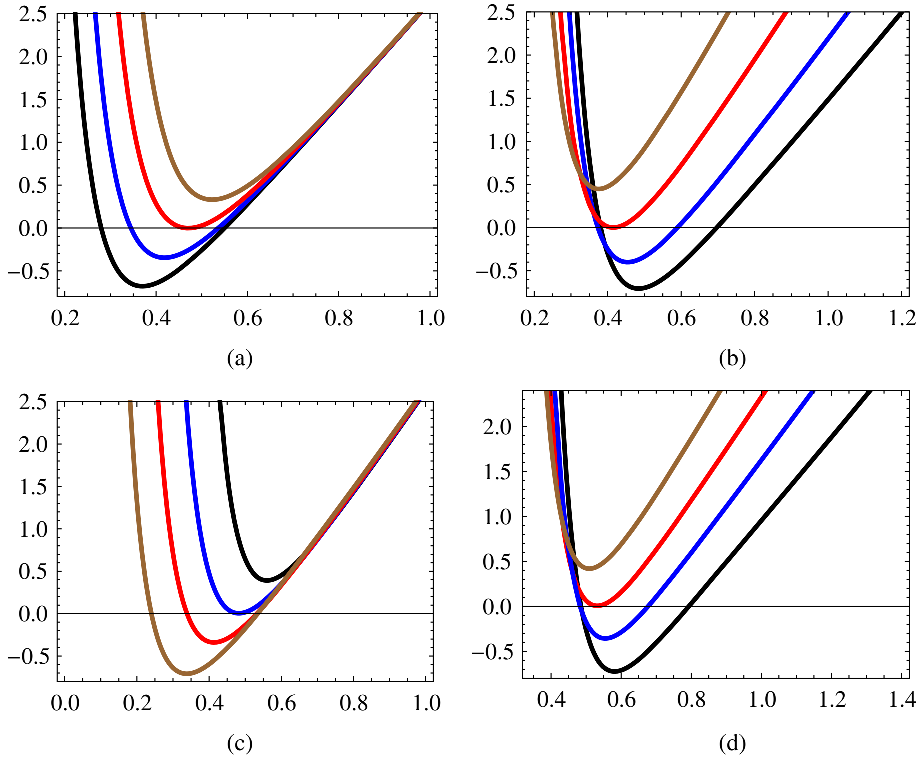

FIG. 1. $W(r)$ vs r for $M=1$, $Q=0.4$, $\Lambda=-3$, $b=2$, and $\beta\neq 1, \sqrt{3}$, Eq. (2.21). (a) $\beta=0.5$, $p=0.7$, and $\alpha=0.45, 0.7, 0.99, 1.3$ for black, blue, red, and brown curves, respectively. (b) $\alpha=0.8$, $p=0.7$, and $\beta=0.48, 0.56, 0.645, 0.72$ for black, blue, red, and brown curves, respectively. (c) $\alpha=0.8$, $\beta=0.6$, and $p=0.62, 0.666, 0.72, 0.8$ for black, blue, red, and brown curves, respectively. (d) $p=0.623$ and $\alpha=\beta=0.4, 0.5, 0.574, 0.64$ for black, blue, red, and brown curves, respectively.

$$\mathcal{R}=ar^{2\beta\gamma-2}+b\frac{W(r)}{r^2}+c\frac{W'(r)}{r}-W''(r), \tag{2.23}$$

$$\mathcal{R}^{\mu\nu\rho\lambda}\mathcal{R}_{\mu\nu\rho\lambda}=\frac{4}{r^{4-4\beta\gamma}}+a_0\frac{W(r)}{r^{4-2\beta\gamma}}+a_1\left(\frac{W(r)}{r^2}\right)^2+a_2\frac{W(r)W'(r)}{r^3}+a_3\left(\frac{W'(r)}{r}\right)^2+(W'')^2, \tag{2.24}$$

where the coefficients a, b, c and a_0, a_1, a_2, and a_3 are functions of dilaton and nonlinearity parameters. Using the metric function (2.21) in Eqs. (2.23) and (2.24), one can see that the Ricci and Kretschmann scalars are finite for finite values of r, and

$$\lim_{r\to\infty}\mathcal{R}=0, \quad \text{and} \quad \lim_{r\to 0}\mathcal{R}=\infty, \tag{2.25}$$

$$\lim_{r\to\infty}\mathcal{R}^{\mu\nu\rho\lambda}\mathcal{R}_{\mu\nu\rho\lambda}=0, \quad \text{and} \quad \lim_{r\to 0}\mathcal{R}^{\mu\nu\rho\lambda}\mathcal{R}_{\mu\nu\rho\lambda}=\infty. \tag{2.26}$$

Equations (2.25) and (2.26) show that there is an essential singularity located at $r=0$ and the asymptotic behavior of the solutions is neither flat nor AdS. It means that inclusion

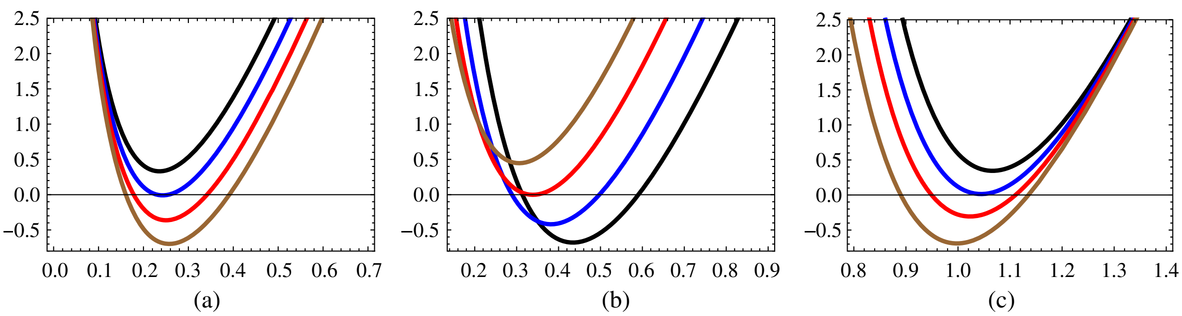

FIG. 2. $W(r)$ vs r for $M=1$, $Q=1.5$, $\Lambda=-3$, $b=1.5$, $L=1$, and $\beta=\sqrt{3}$, Eq. (2.21). (a) $p=0.8$ and $\alpha=0.665, 0.676, 0.688, 0.7$ for black, blue, red, and brown curves, respectively. (b) $\alpha=0.58$ and $p=0.72, 0.735, 0.748, 0.758$ for black, blue, red, and brown curves, respectively. (c) $\alpha=\beta=\sqrt{3}$ and $p=0.62, 0.624, 0.628, 0.633$ for black, blue, red, and brown curves, respectively.

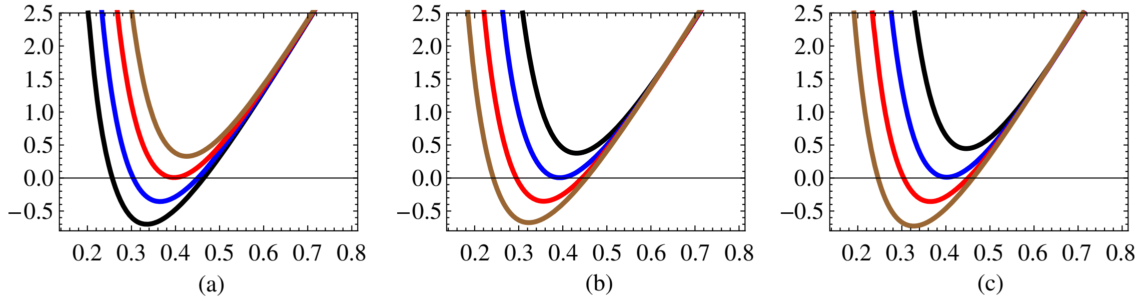

FIG. 3. $W(r)$ vs r for $M = 2.5$, $Q = 0.5$, $\Lambda = -3$, $b = 1.5$, and $\beta = 1$, Eq. (2.21). (a) $p = 0.7$ and $\alpha = 0.84, 1.0, 1.18, 1.35$ for black, blue, red, and brown curves, respectively. (b) $\alpha = 1.3$ and $p = 0.69, 0.718, 0.75, 0.785$ for black, blue, red, and brown curves, respectively. (c) $\alpha = \beta = 1$ and $p = 0.65, 0.675, 0.7, 0.73$ for black, blue, red, and brown curves, respectively.

of the scalar field modifies the asymptotic behavior of the solutions.

It is well known that existence of at least one event horizon and appearance of the curvature singularities are two necessary conditions to be satisfied simultaneously, in order for the solutions to be interpreted as the black holes [45,49,50]. The plots of Figs. 1–3 and Eqs. (2.25) and (2.26) show that both of these requirements are fulfilled by the solutions obtained here. As the result, our new solutions are really black holes.

III. BLACK HOLE THERMODYNAMICS

Now our purpose is to investigate the validity of the first law of black hole thermodynamics for all of the new charged dilatonic black holes obtained in the previous section. So, we find the conserved and thermodynamic quantities related to either of the black hole solutions. The black hole entropy as a pure geometrical quantity can be obtained from the well-known entropy-area law. According to this nearly universal law, which is valid in the Einstein-dilaton gravity theory, the black hole entropy is equal to one quarter of the black hole surface area and for our new black hole solutions can be written in the following form [51,52]:

$$S = \frac{A}{4} = \pi b^2 \left(\frac{b}{r_+}\right)^{2\beta\gamma-2}, \tag{3.1}$$

which reduces to the entropy relation of the Einstein black holes in the absence of dilatonic parameters ($\beta = 0 = \gamma$).

The other thermodynamical quantity which can be calculated geometrically is the Hawking temperature associated with the black hole horizon $r = r_+$. In terms of the surface gravity κ, it can be written as $T = \frac{\kappa}{2\pi}$, with $\kappa = \sqrt{-\frac{1}{2}(\nabla_\mu \chi_\nu)(\nabla^\mu \chi^\nu)} = \frac{1}{2} W'(r_+)$, and χ^μ is null killing vector of the horizon. After some algebraic calculations, we arrived at [32,52]

$$T = \frac{1}{4\pi r_+} \begin{cases} (1+\beta^2)\left[\frac{1}{1-\beta^2}\left(\frac{r_+}{b}\right)^{2\beta\gamma} - \Lambda b^2 \left(\frac{b}{r_+}\right)^{2(\beta\gamma-1)} - \frac{2^{p-1} q^{2p}\Upsilon(\beta)}{b^{2(pB-1)}}\left(\frac{b}{r_+}\right)^{2\eta}\right], & \beta \neq \sqrt{3}, 1, \\ -2\left(\frac{b}{r_+}\right)^{-\frac{3}{2}} - 4\Lambda b^2 \left(\frac{b}{r_+}\right)^{-\frac{1}{2}} - \frac{2^{p+1} q^{2p}\Upsilon(\beta=\sqrt{3})}{b^{2(p\mathcal{B}-1)}}\left(\frac{b}{r_+}\right)^{2\xi}, & \beta = \sqrt{3}, \\ \frac{2r_+}{b}\left[1 - b^2(\Lambda+\lambda_1) + \ln\left(\frac{b}{r_+}\right) - \frac{p 2^{p+2} q^{2p}}{B_1 b^{2(pB_1-1)}}\left(\frac{b}{r_+}\right)^{B_1}\right], & \beta = 1. \end{cases} \tag{3.2}$$

The black hole temperature (3.2) reduces to that of Ref. [42], if one let $p = 1$. Here we have used the relation $W(r_+) = 0$ for eliminating the mass parameter m from the obtained equations. Also, we should mention that extreme black holes occur if $q = q_{\text{ext}}$ and $r_+ = r_{\text{ext}}$ be chosen such that $T = 0$. With this issue in mind and making use of Eq. (3.2), one can show that the extreme black holes exist if the following equations are satisfied:

$$\frac{1}{1-\beta^2} - \Lambda r_{\text{ext}}^2 \left(\frac{b}{r_{\text{ext}}}\right)^{4\beta\gamma} - \frac{2^{p-1} q_{\text{ext}}^{2p} \Upsilon(\beta)}{b^{2(pB-1)}}\left(\frac{b}{r_{\text{ext}}}\right)^{2(\eta+1)} = 0, \quad \text{for } \beta \neq \sqrt{3}, 1, \tag{3.3}$$

$$1 + 2\Lambda b r_{\text{ext}} + \frac{2^p q_{\text{ext}}^{2p} \Upsilon(\beta=\sqrt{3})}{b^{2(p\mathcal{B}-1)}}\left(\frac{b}{r_{\text{ext}}}\right)^{\mathcal{B}-2} = 0, \quad \text{for } \beta = \sqrt{3}, \tag{3.4}$$

$$1 - b^2(\Lambda+\lambda_1) + \ln\left(\frac{b}{r_{\text{ext}}}\right) - \frac{p 2^{p+2} q_{\text{ext}}^{2p}}{B_1 b^{2(pB_1-1)}}\left(\frac{b}{r_{\text{ext}}}\right)^{B_1} = 0, \quad \text{for } \beta = 1. \tag{3.5}$$

In order to study the effects of dilatonic and nonlinearity parameters (i.e., α, β and p) on the horizon temperature of the black holes, the plots of black hole temperature vs horizon radius have been shown in Figs. 4–6 by considering the $\alpha = \beta$ and $\alpha \neq \beta$ cases, separately. The plots of Figs. 4 and 6 show that, in the cases $\beta \neq \sqrt{3}, 1$ and $\beta = 1$, the extreme black holes can occur for $r_+ = r_{\rm ext}$ only. Also, the physical black holes with positive temperature are those for which $r_+ > r_{\rm ext}$ and unphysical black holes, having negative temperature, occur if $r_+ < r_{\rm ext}$. Regarding the plots of Fig. 5 (for black holes with $\beta = \sqrt{3}$), one can argue that the equation $T = 0$ has two real roots located at $r_+ = r_{1{\rm ext}}$ and $r_+ = r_{1{\rm ext}}$, where the extreme black holes can occur. The black holes are physically acceptable if their horizon radii be in the range $r_{1{\rm ext}} < r_+ < r_{2{\rm ext}}$.

We can find the electric potential Φ of black holes, measured by an observer located at infinity with respect to the horizon, using the following relation [46,53–55]:

$$\Phi = A_\mu \chi^\mu|_{\rm reference} - A_\mu \chi^\mu|_{r=r_+}. \tag{3.6}$$

Here, $\chi = C\partial_t$ is the null generator of the horizon and C is an arbitrary constant to be determined [43,44]. Using Eqs. (2.14) and (3.6), one can find the black hole's electric potential on the horizon as

$$\Phi = \frac{Cq}{B-1} r_+^{1-B}. \tag{3.7}$$

By calculating the total electric flux measured by an observer located at infinity with respect to the horizon (i.e., $r \to \infty$) [50,56], we can find the conserved electric charge of the black holes. It can be obtained with the help of Gauss's electric law which can be written as [43,57]

$$Q = \frac{1}{4\pi}\int_{r\to\infty} r^2 e^{2\beta\phi(r)} (-\mathcal{F})^{p-1} e^{-2p\alpha\phi(r)} F_{\mu\nu} u^\mu u^\nu d\Omega, \tag{3.8}$$

where u_μ and u_ν are timelike and spacelike unit vectors normal to the hypersurface of radius r, respectively. Making use of Eqs. (2.2), (2.13), and (2.14), after some simple calculations, we arrived at

$$Q = 2^{p-1} b^2 \left(\frac{q}{b^B}\right)^{2p-1}, \tag{3.9}$$

which is compatible with the results of our previous work in the case $p = 1$ [42]. It reduces to the charge of Reissner-Nordström-A(dS) black holes in the absence of dilatonic field. Also, a redefinition of the integration constant q makes this relation consistent with the result of Refs. [46,57].

The other conserved quantity to be calculated is the black hole mass. As mentioned before, it can be obtained in terms of the mass parameter m. Since the asymptotic behavior of the metric functions given by Eq. (2.21) is unusual, the Brown and York quasilocal formalism must be used for obtaining the quasilocal mass [58,59]. By considering a metric in the following form (Eq. (2.7) in Ref. [60]):

$$ds^2 = -X^2(\rho)dt^2 + \frac{d\rho^2}{Y^2(\rho)} + \rho^2(d\theta^2 + \sin^2\theta d\varphi^2), \tag{3.10}$$

provided that the matter field does not contain derivatives of the metric, the quasilocal black hole mass can be obtained through the following relation (Eq. (2.8) in Ref. [60]):

$$\mathcal{M} = \rho X(\rho)[Y_0(\rho) - Y(\rho)], \tag{3.11}$$

in which $Y_0(\rho)$ is a background metric function which determines the zero of the mass.

In order to obtain the analogous Arnowitt-Deser-Misner (ADM) mass M, the limit $\rho \to \infty$ must be taken [60]. Now, we must to write the metric (2.6) in the form of Eq. (3.10). This can be done by considering the transformation $\rho = rR(r)$, from which one can show that

$$dr^2 = \frac{d\rho^2}{(1-\beta\gamma)^2 R^2(r)}.$$

Therefore, in our case, we have

$$X^2(\rho) = W(r), \quad \text{and} \quad Y^2(\rho) = \frac{R^2(r)}{(1+\beta^2)^2} W(r), \quad \text{with} \quad r = r(\rho). \tag{3.12}$$

By substituting these quantities into Eq. (3.11) and taking the limit $\rho \to \infty$ or equivalently $r \to \infty$, the total mass of the charged dilatonic black holes, identified here, is obtained as (see the Appendix)

$$M = \frac{mb^{2\beta\gamma}}{2(1+\beta^2)}, \tag{3.13}$$

which is compatible with the result of Refs. [37,42,46]. Also, it recovers the mass of Reissner-Nordström-A(dS) black holes when the dilatonic potential disappears.

Now, we can investigate the consistency of these quantities with the thermodynamical first law. From Eqs. (2.21), (3.1), (3.9), and (3.13), we can obtain the black hole mass as the function of extensive parameters S and Q. To do so, we use the relation $W(r_+) = 0$. The Smarr-type mass formula for the new black holes can be given as

$$M(r_+,q)=\begin{cases}\frac{b}{2}\left[\frac{1}{1-\beta^2}\frac{r_+}{b}-\frac{\Lambda b^2(1+\beta^2)}{3-\beta^2}\left(\frac{b}{r_+}\right)^{4\beta\gamma-3}+\frac{2^{p-1}q^{2p}\Upsilon(\beta)}{(\mathcal{B}-1)b^{2(p\mathcal{B}-1)}}\left(\frac{b}{r_+}\right)^{2\eta+2\beta\gamma-1}\right], & \beta\neq 1,\sqrt{3},\\ -\frac{b}{4}\left[\frac{r_+}{b}+2\Lambda b^2\ln\left(\frac{r_+}{L}\right)-\frac{2^pq^{2p}\Upsilon(\beta=\sqrt{3})}{(\mathcal{B}-1)b^{2(p\mathcal{B}-1)}}\left(\frac{b}{r_+}\right)^{\frac{1}{2}(\sqrt{3}\alpha-1)}\right], & \beta=\sqrt{3},\\ \frac{b}{2}\left\{\left[2-b^2(\Lambda+\lambda_1)+\ln\left(\frac{b}{r_+}\right)\right]\left(\frac{r_+}{b}\right)+\frac{p2^pq^{2p}}{B_1(B_1-1)b^{2(pB_1-1)}}\left(\frac{b}{r_+}\right)^{B_1-1}\right\}, & \beta=1.\end{cases}\qquad(3.14)$$

It is a matter of calculation to show that the intensive parameters T and Φ, conjugate to the black hole entropy and charge, satisfy the following relations:

$$\left(\frac{\partial M}{\partial S}\right)_Q=T,\quad\text{and}\quad\left(\frac{\partial M}{\partial Q}\right)_S=\Phi,\qquad(3.15)$$

provided that C be chosen as [44]

$$C=\begin{cases}\frac{p(2-\Upsilon_1)}{1+\alpha p} & \text{for } \beta=1,\\ \frac{p\Upsilon(\beta)}{2p-1} & \text{for } \beta\neq 1.\end{cases}\qquad(3.16)$$

Note that $\Upsilon_1=(\alpha p-2p+1)(\alpha p-2p+2)(2p-1)^{-1}$ and the condition $r_+=b$ has been used for the case $\beta=1$. Also, Eq. (3.16) reduces to its corresponding value in the Einstein-Maxwell-dilaton gravity theory [42]. So, we showed that the first law of black hole thermodynamics is valid, for all of the new nonlinearly charged dilatonic black holes, in the following form:

$$dM(S,Q)=TdS+\Phi dQ.\qquad(3.17)$$

Here, S and Q are the thermodynamical extensive parameters and T and Φ are intensive parameters conjugate to S and Q, respectively. From Eq. (3.17), one can argue that even if the conserved and thermodynamic quantities are affected by dilaton and nonlinearity parameters, the first law of black hole thermodynamics remains valid.

IV. BLACK HOLE LOCAL STABILITY

Now, using the canonical ensemble method, we study the thermal stability or phase transition of our new black hole solutions. For this purpose, we need to calculate the black hole heat capacity with the black hole charge as a constant. It is defined as

$$C_Q=T\left(\frac{\partial S}{\partial T}\right)_Q=\frac{T}{M_{SS}}.\qquad(4.1)$$

The last step in Eq. (4.1) comes from the fact that $T=(\partial M/\partial S)_Q$ and we have used the definition $M_{SS}=(\partial^2M/\partial S^2)_Q$.

It is well known that the positivity of the black hole heat capacity C_Q or equivalently the positivity of $(\partial S/\partial T)_Q$ or M_{SS} is sufficient to ensure the local stability of the physical black holes. The unstable black holes undergo phase transitions to be stabilized. The sign of the black hole heat capacity changes, from negative to positive, at its vanishing points. Thus, they signal the existence of a kind of phase transition. In addition, an unstable black hole undergoes phase transition at the divergent points of the black hole heat capacity where the denominator of the heat capacity vanishes. These two kinds of thermodynamic phase transitions are called as type-1 and type-2 phase transitions, respectively [61–63] (see also [45,52,64]). Considering the abovementioned points, we proceed to perform a thermal stability or phase transition analysis for all of the new black hole solutions we just obtained.

A. Black holes with $\beta\neq 1,\sqrt{3}$

Making use of Eq. (3.14) and noting Eq. (3.1), the denominator of the black hole heat capacity can be calculated as

$$M_{SS}=\frac{-(1+\beta^2)}{8\pi^2b^3}\left(\frac{b}{r_+}\right)^{1-2\beta\gamma}\left[\left(\frac{b}{r_+}\right)^{2-2\beta\gamma}+\Lambda b^2(1-\beta^2)\left(\frac{b}{r_+}\right)^{2\beta\gamma}-\frac{2^{p-1}q^{2p}\Upsilon(\beta)}{b^{2(p\mathcal{B}-1)}}\left(\frac{b}{r_+}\right)^{2\eta+2}\right].\qquad(4.2)$$

The real roots of equation $M_{SS}=0$ indicate the points of type-2 phase transition. As it is too difficult to obtain the real roots of this equation analytically, we have plotted M_{SS} vs r_+ in Fig. 4 for different values of dilaton and nonlinearity parameters. The plots show that, for the properly fixed parameters, M_{SS} is positive valued everywhere and no type-2 phase transition can take place. This kind of black holes undergo type-1 phase transition at the point $r_+=r_{\mathrm{ext}}$ where the black hole heat capacity vanishes. The black holes with the horizon radii in the range $r_+>r_{\mathrm{ext}}$ are locally stable.

B. Black holes with $\beta=\sqrt{3}$

The numerator of these black holes is given by Eq. (3.2). Also, it is a matter of calculation to show that its denominator is given by the following equation:

$$M_{SS}=\frac{-1}{2\pi^2b^3}\left[1-2\Lambda b^2\left(\frac{b}{r_+}\right)-\frac{2^pq^{2p}(2\mathcal{B}-1)\Upsilon(\beta=\sqrt{3})}{b^{2(p\mathcal{B}-1)}}\left(\frac{b}{r_+}\right)^{\mathcal{B}}\right].\qquad(4.3)$$

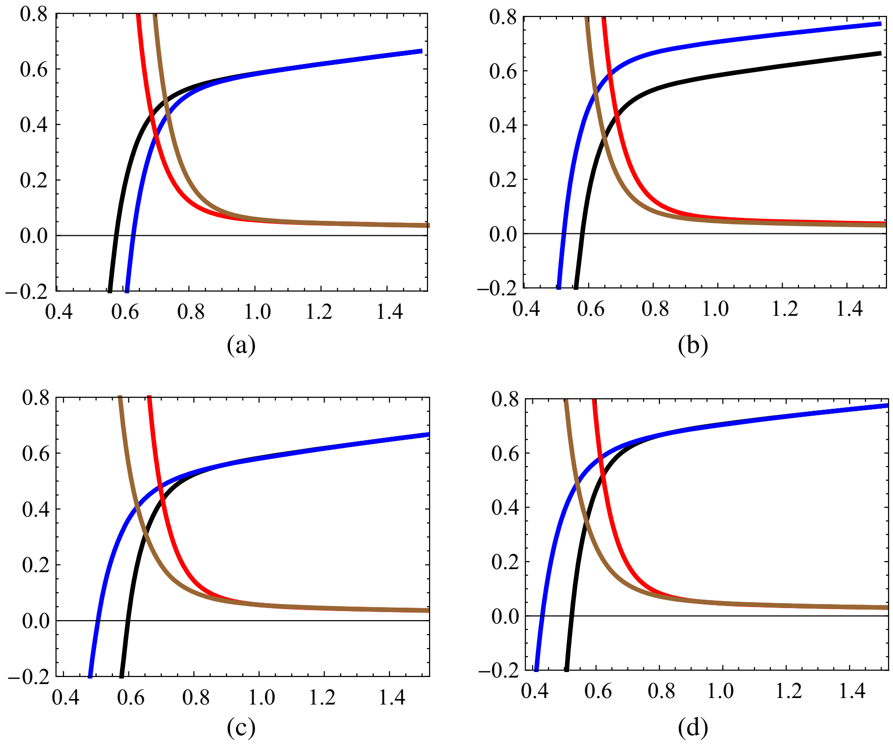

FIG. 4. T and M_{SS} vs r_+ for $Q = 0.4$, $\Lambda = -3$, $b = 2$, and $\beta \neq 1, \sqrt{3}$, Eqs. (3.2) and (4.2). (a) $\beta = 0.6$, $p = 0.7$ and $[T\colon \alpha = 0.7(\text{black}), 1.0(\text{blue})]$ and $[2M_{SS}\colon \alpha = 0.7(\text{red}), 1.0(\text{brown})]$. (b) $\alpha = 0.7$, $p = 0.6$ and $[T\colon \beta = 0.6(\text{black}), 0.7(\text{blue})]$ and $[2M_{SS}\colon \alpha = 0.6(\text{red}), 0.7(\text{brown})]$. (c) $\alpha = 0.8$, $\beta = 0.6$ and $[T\colon p = 0.6(\text{black}), 0.65(\text{blue})]$ and $[2M_{SS}\colon p = 0.6(\text{red}), 0.65(\text{brown})]$. (d) $\alpha = \beta = 0.7$ and $[T\colon p = 0.6(\text{black}), 0.65(\text{blue})]$ and $[2M_{SS}\colon p = 0.6(\text{red}), 0.65(\text{brown})]$.

The plots of denominator together with the numerator of the black hole heat capacity are shown in Fig. 5 for different values of nonlinearity and dilaton parameters. Regarding the plots of Fig. 5, it is easily understood that there are two points of type-1 phase transition located at the points $r_+ = r_{1\text{ext}}$ and $r_+ = r_{2\text{ext}}$ with $r_{1\text{ext}} < r_{2\text{ext}}$. The black hole heat capacity diverges at the real root of $M_{SS} = 0$, which appears at the point $r_+ = r_0$ with $r_0 < r_{1\text{ext}}$. Also, the physical black holes, those having positive temperature, are unstable everywhere. Because their horizon radius is in the range $r_{1\text{ext}} < r_+ < r_{2\text{ext}}$ and they have negative heat capacity in this range.

C. Black holes with $\beta = 1$

Starting from Eq. (3.14) and using Eq. (3.1), one can calculate the denominator of the black hole heat capacity. It can be written in the following form:

$$M_{SS} = \frac{-1}{2\pi^2 b^2 r_+}\left[1 - \frac{p 2^p q^{2p}}{b^{2(pB_1-1)}}\left(\frac{b}{r_+}\right)^{B_1}\right]. \tag{4.4}$$

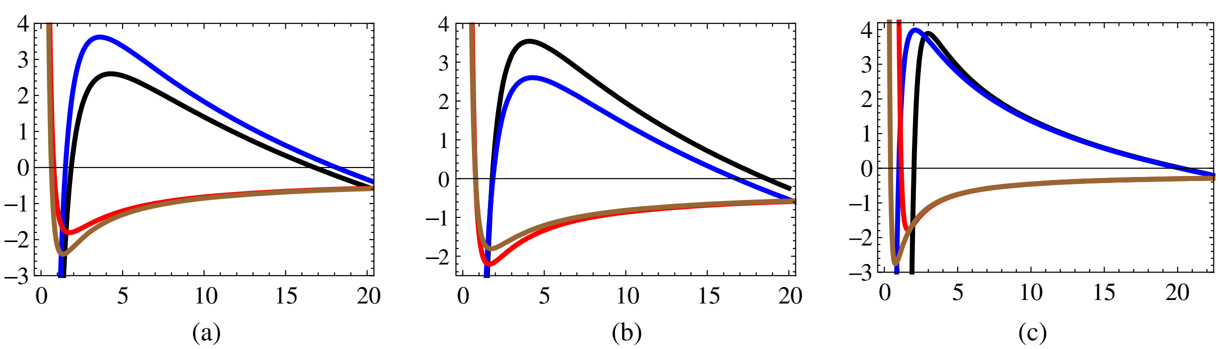

FIG. 5. T and M_{SS} vs r_+ for $Q = 2.5$, $\Lambda = -3$, $b = 1.5$, and $\beta = \sqrt{3}$, Eqs. (3.2) and (4.3). (a) $p = 0.8$ and $[10T\colon \alpha = 0.8(\text{black}), 0.9(\text{blue})]$ and $[20M_{SS}\colon \alpha = 0.8(\text{red}), 0.9(\text{brown})]$. (b) $\alpha = 0.8$ and $[10T\colon p = 0.75(\text{black}), 0.8(\text{blue})]$ and $[20M_{SS}\colon p = 0.75(\text{red}), 0.8(\text{brown})]$. (c) $\alpha = \beta = \sqrt{3}$ and $[5T\colon p = 0.6(\text{black}), 0.8(\text{blue})]$ and $[10M_{SS}\colon p = 0.6(\text{red}), 0.8(\text{brown})]$.

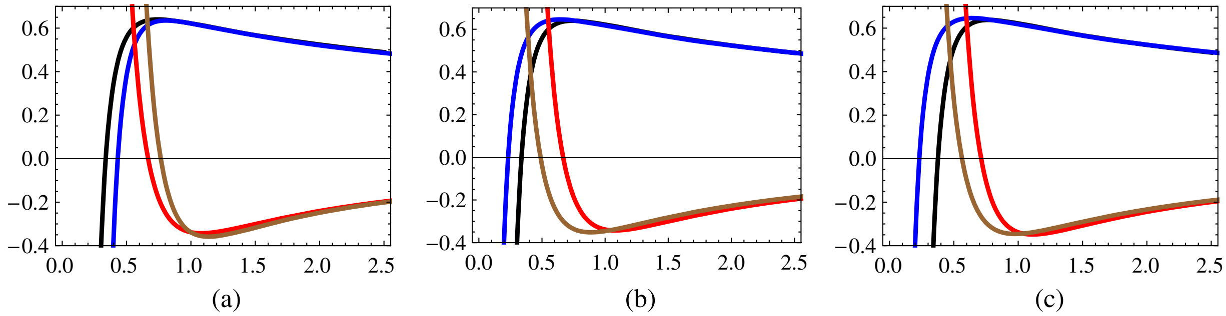

FIG. 6. T and M_{SS} vs r_+ for $Q = 0.4$, $\Lambda = -3$, $b = 2$, and $\beta = 1$, Eqs. (3.2) and (4.4). (a) $p = 0.7$ and [T: $\alpha = 0.7$(black), 1.5(blue)] and [$10M_{SS}$: $\alpha = 0.7$(red), 1.5(brown)]. (b) $\alpha = 0.7$ and [T: $p = 0.7$(black), 0.8(blue)] and [$10M_{SS}$: $p = 0.7$(red), 0.8(brown)]. (c) $\alpha = \beta = 1$ and [T: $p = 0.7$(black), 0.8(blue)] and [$10M_{SS}$: $p = 0.7$(red), 0.8(brown)].

In order to investigate the points of type-1 and type-2 phase transitions and to determine the ranges at which the black hole heat capacity is positive valued, we have plotted the numerator and denominator of the black hole heat capacity in Fig. 6. The plots show that there is a point of type-1 phase transition located at $r_+ = r_{\rm ext}$, where the black hole heat capacity vanishes. The black hole heat capacity diverges at $r_+ = r_1$ and it is point of type-2 phase transition. This kind of black holes are locally stable provided that the condition $r_{\rm ext} < r_+ < r_1$ is fulfilled.

V. BLACK HOLE GLOBAL STABILITY

Study of the black hole global stability was initially proposed by Hawking and Page, as the pioneers of this idea [65]. Based on this proposal, one can investigate the global stability of black holes by studying the corresponding Gibbs free energy. The Gibbs free energy of the charged black holes in the grand canonical ensemble is given by [66]

$$G = M - TS - Q\Phi. \tag{5.1}$$

The Gibbs free energy is required to be positive to ensure global stability of the black holes with positive temperature. The Hawking-Page phase transition can occur at the points where the Gibbs free energy vanishes. The black hole temperature at which the Hawking-Page phase transition takes place is dubbed as the critical temperature (T_H). At this temperature, Hawking-Page phase transition between black hole and thermal state (radiation) occurs [65–67]. In the following subsections, we calculate the Gibbs free energy of our new black holes and, regarding the abovementioned points, analyze their global stability.

A. Black holes with $\beta \neq 1, \sqrt{3}$

Noting Eqs. (3.1), (3.2), (3.7), (3.9), (3.14), and (5.1), after some algebraic calculations, we arrive the Gibbs free energy as follows:

$$G = \frac{r_+}{4} + \frac{\Lambda b^3(1-\beta^4)}{4(3-\beta^2)}\left(\frac{b}{r_+}\right)^{4\beta\gamma-3} - \frac{2^{p-1}q^{2p}\Upsilon(\beta)r_+}{(B-1)b^{2(pB-1)}}\left[\frac{p}{2p-1}\left(\frac{b}{r_+}\right)^{B} - \frac{1}{4}\{1-\beta^2+B(1+\beta^2)\}\left(\frac{b}{r_+}\right)^{2\eta+2\beta\gamma}\right]. \tag{5.2}$$

We need the real roots of equation $G(r_+) = 0$, but this is a difficult task analytically. So we plot the curves of G in terms of r_+. They are shown in Fig. 7. It is seen from Fig. 7 that at the vanishing point of Gibbs free energy labeled by $r_+ = r_c$, the Hawking-Page phase transition occurs. For $r_{\rm ext} < r_+ < r_c$, where both the Gibbs free energy and temperature are positive, the black hole is globally stable. In $r_+ = r_{\rm ext}$, the temperature is zero (extremal black hole) but in $r_+ = r_c$ temperature is equal to T_H at which the Gibbs free energy vanishes. We should mention that in the range $r_{\rm ext} < r_+ < R_c$ the Gibbs free energy is a decreasing function of r_+. So the larger black holes are more stable ones.

B. Black holes with $\beta = \sqrt{3}$

By use of the expressions presented in Eqs. (3.1), (3.2), (3.7), (3.9), and (3.14) into Eq. (5.1), we obtain the Gibbs free energy of the black holes correspond to the case $\beta = \sqrt{3}$. That is

$$G = \frac{r_+}{4} + \Lambda b^3\left\{1 - \frac{1}{2}\ln\left(\frac{r_+}{L}\right)\right\} + \frac{2^{p-2}q^{2p}\Upsilon(\beta=\sqrt{3})}{(\mathcal{B}-1)b^{2(p\mathcal{B}-1)}}r_+\left[\left(\frac{b}{r_+}\right)^{\frac{1}{2}(\sqrt{3}\alpha+1)} + 2(\mathcal{B}-1)\left(\frac{b}{r_+}\right)^{2\xi+\frac{3}{2}} - \frac{2p}{2p-1}\left(\frac{b}{r_+}\right)^{\mathcal{B}}\right]. \tag{5.3}$$

As it is difficult to solve the equation $G(r_+) = 0$ and obtain its real roots analytically, we have shown the plots of G and T vs r_+ in Fig. 8.

The plots of Fig. 8 show that the Gibbs free energy of this class of black holes vanishes at $r_+ = r_{c1}$, and black holes with horizon radius equal to r_{c1} experience Hawking-Page phase transition. The black holes with horizon radius

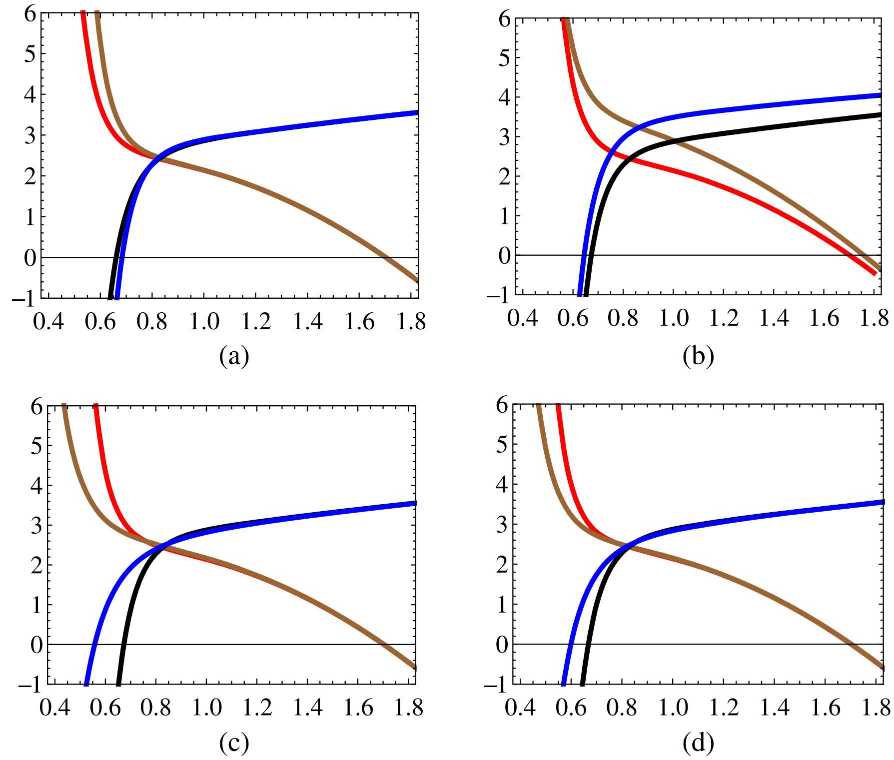

FIG. 7. T and G vs r_+ for $q = 1$, $\Lambda = -3$, $b = 2$, and $\beta \neq 1, \sqrt{3}$, Eqs. (3.2) and (5.2). (a) $\beta = 0.6$, $p = 0.6$ and [$5T$: $\alpha = 0.4$(black), 1.2(blue)] and [G: $\alpha = 0.4$(red), 1.2(brown)]. (b) $\alpha = 0.8$, $p = 0.6$ and [$5T$: $\beta = 0.6$(black), 0.8(blue)] and [G: $\beta = 0.6$(red), 0.8(brown)]. (c) $\alpha = 0.8$, $\beta = 0.6$ and [$5T$: $p = 0.6$(black), 0.7(blue)] and [G: $p = 0.6$(red), 0.7(brown)]. (d) $\alpha = \beta = 0.6$ and [$5T$: $p = 0.6$(black), 0.65(blue)] and [G: $p = 0.6$(red), 0.65(brown)].

in the range $r_{c1} < r_+ < r_{2\mathrm{ext}}$ are globally stable. Since the Gibbs free energy is an increasing function of r_+, the smaller black holes with the horizon radius in this range are more stable. For the black holes with the horizon radius smaller than r_{c1}, the thermal/or radiation state is preferred.

C. Black holes with $\beta = 1$

Through combination of Eqs. (3.1), (3.2), (3.7), (3.9), (3.14), and (5.1), one is able to show that the Gibbs free energy of this kind of black holes, as the function of black hole horizon radius, can be written in the following form:

$$G = \frac{r_+}{2} + \frac{p 2^{p-1} q^{2p} r_+}{B_1 (B_1 - 1) b^{2(pB_1 - 1)}} \times \left\{ 4B_1 - 3 - \frac{(2 - \Upsilon_1) B_1}{(1 + \alpha p)} \right\} \left(\frac{b}{r_+} \right)^{B_1}. \tag{5.4}$$

For the purpose of global stability analysis of the black holes, we have plotted G and T vs r_+ in Fig. 9.

The plots of Fig. 9 show that there is a critical radius at which Gibbs free energy vanishes which we label by r_{c2}. The black holes with horizon radius equal to r_{c2} undergo Hawking-Page phase transition. This kind of black holes

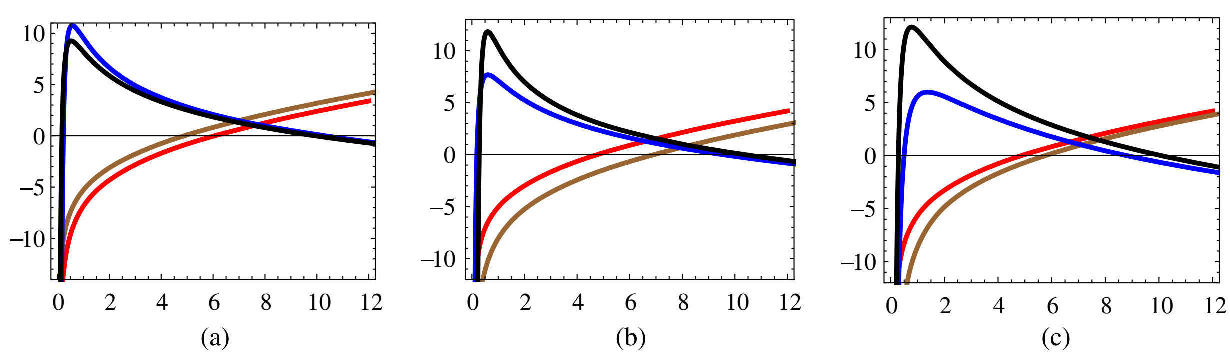

FIG. 8. T and G vs r_+ for $q = 1.2$, $\Lambda = -3$, $b = 1.2$, and $\beta = \sqrt{3}$, Eqs. (3.2) and (5.3). (a) $p = 0.75$ and [$10T$: $\alpha = 0.6$(black), 1.0(blue)] and [G: $\alpha = 0.6$(red), 1.0(brown)]. (b) $\alpha = 0.7$ and [$10T$: $p = 0.65$(black), 0.8(blue)] and [G: $p = 0.65$(red), 0.8(brown)]. (c) $\alpha = \beta = \sqrt{3}$ and [$10T$: $p = 1.0$(black), 1.2(blue)] and [G: $p = 1$(red), 1.2(brown)].

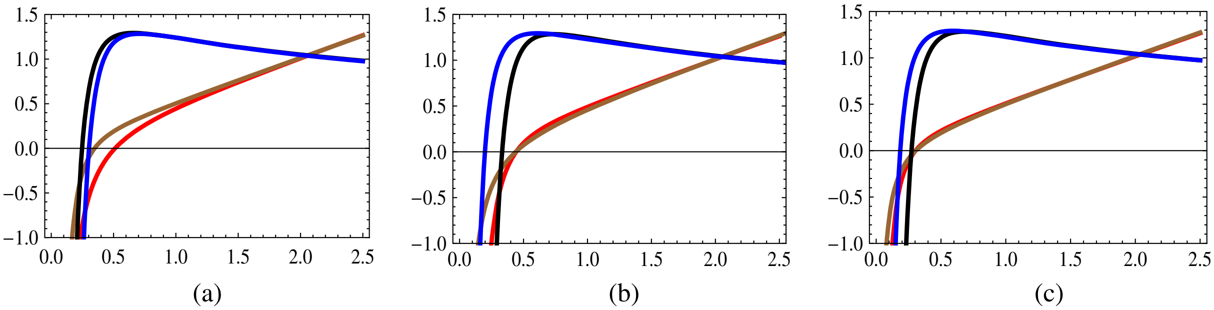

FIG. 9. T and G vs r_+ for $q = 0.4$, $\Lambda = -3$, $b = 1$, and $\beta = 1$, Eqs. (3.2) and (5.4). (a) $p = 0.75$ and $[2T\colon\ \alpha = 0.5(\text{black}), 0.9(\text{blue})]$ and $[G\colon\ \alpha = 0.5(\text{red}), 0.9(\text{brown})]$. (b) $\alpha = 0.7$ and $[2T\colon\ p = 0.7(\text{black}), 0.85(\text{blue})]$ and $[G\colon\ p = 0.7(\text{red}), 0.85(\text{brown})]$. (c) $\alpha = \beta = 1$ and $[2T\colon\ p = 0.8(\text{black}), 0.95(\text{blue})]$ and $[G\colon\ p = 0.8(\text{red}), 0.95(\text{brown})]$.

with the horizon radius greater than r_{c2} are globally stable. The Gibbs free energy is an increasing function of r_+; therefore, the black holes with smaller horizon radius are more stable. In addition, the black holes with the horizon radius in the range $r_{\text{ext}} < r_+ < r_{c2}$ prefer the thermal state.

VI. CONCLUSION

In this work, we have studied thermodynamic properties of the new nonlinearly charged dilatonic four-dimensional black holes, as the exact solutions to the field equations of the Einstein-power-Maxwell-dilaton gravity theory. The explicit form of the coupled scalar, electromagnetic, and gravitational field equations has been obtained by varying the action of Einstein-dilaton gravity coupled to power-Maxwell invariant as the matter field. By introducing a static and spherically symmetric geometry, we found that the solution of the scalar field equation can be written in the form of a generalized Liouville dilatonic potential. Also, three new classes of charged dilaton black hole solutions have been obtained in the presence of the power law nonlinear electrodynamics. By considering Ricci and Kretschmann scalars, we found that there is a point of essential singularity located at the origin. Also, the asymptotic behavior of the solutions is neither flat nor AdS. The existence of the real roots of the metric functions together with the singular Ricci and Kretschmann scalars is sufficient to interpret the solutions as black hole. Plots of Figs. 1–4, show that the new black hole solutions can provide two horizon, extreme and naked singularity black holes for the suitably fixed parameters.

Then, we studied the thermodynamics of the new black hole solutions. We have obtained the conserved charge and mass of the black holes. Using the geometrical approaches, we have calculated the temperature, entropy, and electric potential for all of the new black hole solutions. We showed that for the black hole solutions with $\beta \neq 1$, $\sqrt{3}$, and $\beta = 1$ the extreme, physical, and unphysical black holes can occur if $r_+ = r_{\text{ext}}$, $r_+ > r_{\text{ext}}$, and $r_+ < r_{\text{ext}}$, respectively, while for those with $\beta = \sqrt{3}$ the extreme black holes occur at the points $r_+ = r_{1\text{ext}}$ and $r_+ = r_{2\text{ext}}$. The radii of physical black holes are in the range $r_{1\text{ext}} < r_+ < r_{2\text{ext}}$ and unphysical black holes are in the ranges $r_+ < r_{1\text{ext}}$ and $r_+ > r_{2\text{ext}}$. Using a Smarr-type mass formula, we have found the black hole mass as the function of the thermodynamical extensive parameters S and Q, from which we have obtained the intensive parameters T and Φ. Compatibility of the results obtained from thermodynamical and geometrical methods proves the validity of the thermodynamical first law for all of the new black hole solutions.

Then, from the canonical ensemble point of view, we have studied the thermal stability or phase transition of the new black hole solutions. Regarding the signature of the black hole heat capacity with the black hole charge as a constant, we obtained that the following possibilities are considerable. (i) For the heat capacity of the black holes with $\beta \neq 1$, $\sqrt{3}$, there is no divergent point and no type-2 phase transition occur. Type-1 phase transition takes place at the point $r_+ = r_{\text{ext}}$ where the black hole heat capacity vanishes. This class of black holes remain stable for the horizon radii in the range $r_+ > r_{\text{ext}}$ (Fig. 4). (ii) The black holes corresponding to $\beta = \sqrt{3}$ have two points of type-1 phase transition labeled by $r_+ = r_{1\text{ext}}$ and $r_+ = r_{1\text{ext}}$ which are the real roots of $T = 0$. There is a point of type-2 phase transition located at $r_+ = r_0$, at which the black hole heat capacity diverges. The physical black holes with positive temperature are unstable (Fig. 5). (iii) As it is shown in Fig. 6, the black holes with $\beta = 1$ undergo type-2 phase transition at the divergent point of black hole heat capacity labeled by $r_+ = r_1$. There is point of type-1 phase transition located at $r_+ = r_{\text{ext}}$ where the black hole heat capacity vanishes. This class on new black hole solutions is stable provided that their horizon radii be in the range $r_{\text{ext}} < r_+ < r_1$.

Finally, making use of the grand canonical ensemble and noting the Gibbs free energy of the black holes, we analyzed the global stability of the new black holes obtained here. We determined the points at which the black holes experience Hawking-Page phase transition. Also we showed that there are some specific intervals for the horizon radii in such a way that the black holes with the horizon radius in this intervals are globally stable (Figs. 7–9).

ACKNOWLEDGMENTS

The authors appreciate the Research Council of Razi University for official support of this work.

APPENDIX: DETAILED DERIVATION OF EQ. (3.13)

With the purpose of finding the black hole mass for ththis terme spherically symmetric black holes, with the nonflat and non-AdS asymptotic behavior identified in this work, we start by substituting the metric function $W(r)$ into Eqs. (3.11) and (3.12). To do this, we consider the cases corresponding to the $\beta \neq 1,\ \sqrt{3},\ \beta = \sqrt{3}$, and $\beta = 1$, separately.

1. The case $\beta \neq 1, \sqrt{3}$

In this case, the quasilocal black hole mass can be obtained as follows:

$$\mathcal{M} = r\left(\frac{b}{r}\right)^{2\beta\gamma}(1-\beta\gamma)[\{[-mr^{2\beta\gamma-1}+u(r)]u(r)\}^{1/2}+mr^{2\beta\gamma-1}-u(r)], \tag{A1}$$

in which

$$u(r) = \frac{1+\beta^2}{1-\beta^2}\left(\frac{r}{b}\right)^{2\beta\gamma} - \frac{\Lambda b^2(1+\beta^2)^2}{3-\beta^2}\left(\frac{r}{b}\right)^{\frac{2\gamma}{\beta}} + \frac{q^{2p}2^{p-1}(1+\beta^2)\Upsilon(\beta)}{(B-1)b^{2(^pB-1)}}\left(\frac{b}{r}\right)^{2\eta}. \tag{A2}$$

Now, Eq. (A1) can be rewritten as

$$\begin{aligned}
\mathcal{M} &= (1-\beta\gamma)b^{2\beta\gamma}r^{1-2\beta\gamma}\left[u(r)\left\{1-\frac{mr^{2\beta\gamma-1}}{u(r)}\right\}^{1/2}+mr^{2\beta\gamma-1}-u(r)\right],\\
&= \frac{b^{2\beta\gamma}}{1+\beta^2}r^{1-2\beta\gamma}\left[u(r)\left\{1-\frac{mr^{2\beta\gamma-1}}{2u(r)}-\frac{1}{8}\left(\frac{mr^{2\beta\gamma-1}}{u(r)}\right)^2+\mathcal{O}\left(\frac{r^{2\beta\gamma-1}}{u(r)}\right)^3\right\}+mr^{2\beta\gamma-1}-u(r)\right],\\
&= \frac{b^{2\beta\gamma}}{1+\beta^2}r^{1-2\beta\gamma}\left[u(r)-\frac{mr^{2\beta\gamma-1}}{2}-\frac{u(r)}{8}\left(\frac{mr^{2\beta\gamma-1}}{u(r)}\right)^2+r^{2\beta\gamma-1}\mathcal{O}\left(\frac{r^{2\beta\gamma-1}}{u(r)}\right)^2+mr^{2\beta\gamma-1}-u(r)\right],\\
&= \frac{b^{2\beta\gamma}}{1+\beta^2}\left[\frac{m}{2}-\frac{m^2}{8}\left(\frac{r^{2\beta\gamma-1}}{u(r)}\right)+\mathcal{O}\left(\frac{r^{2\beta\gamma-1}}{u(r)}\right)^2\right].
\end{aligned} \tag{A3}$$

Thus, the black hole mass can be calculated as

$$M = \lim_{r\to\infty}\mathcal{M} = \lim_{r\to\infty}\frac{b^{2\beta\gamma}}{1+\beta^2}\left[\frac{m}{2}-\frac{m^2}{8}\left(\frac{r^{2\beta\gamma-1}}{u(r)}\right)+\mathcal{O}\left(\frac{r^{2\beta\gamma-1}}{u(r)}\right)^2\right]. \tag{A4}$$

It is easily shown that $\lim_{r\to\infty}(\frac{r^{2\beta\gamma-1}}{u(r)})$ and its higher powers are equal to zero. As the result, one obtains

$$M = \frac{b^{2\beta\gamma}}{1+\beta^2}\frac{m}{2}. \tag{A5}$$

2. The case $\beta = \sqrt{3}$

In this case, regarding Eqs. (2.21) and (3.11), the black hole quasilocal mass is obtained as

$$\mathcal{M} = \frac{1}{4}b^{\frac{3}{2}}r^{-\frac{1}{2}}[\{[-mr^{\frac{1}{2}}+u_3(r)]u_3(r)\}^{1/2}+mr^{\frac{1}{2}}-u_3(r)], \tag{A6}$$

$$u_3(r) = -2\left(\frac{r}{b}\right)^{2/3} - 4\Lambda(b^3r)^{\frac{1}{2}}\ln\left(\frac{r}{L}\right) + \frac{2^{p+1}q^{2p}\Upsilon(\beta=\sqrt{3})}{(\mathcal{B}-1)b^{2(^p\mathcal{B}-1)}}\left(\frac{b}{r}\right)^{2\xi}. \tag{A7}$$

Making use of the binomial expansion relation, after some algebraic simplifications, we arrive at

$$\mathcal{M} = \frac{b^{\frac{3}{2}}}{8} - \frac{m^2b^{\frac{3}{2}}}{32}\left(\frac{r^{\frac{1}{2}}}{u_3(r)}\right) + \mathcal{O}\left(\frac{r^{\frac{1}{2}}}{u_3(r)}\right)^2. \tag{A8}$$

Taking limit $r\to\infty$, results in

$$M = \frac{mb^{\frac{3}{2}}}{8}. \tag{A9}$$

3. The case $\beta = 1$

Noting Eq. (3.11) the quasilocal mass of the black holes, with the metric function given by Eq. (2.21), can be written in the following form:

$$\mathcal{M} = \frac{b}{2}\left[u_1(r)\left\{1 - \frac{m}{u_1(r)}\right\}^{1/2} + m - u_1(r)\right], \tag{A10}$$

with

$$u_1(r) = 2\left[2 - b^2(\Lambda + \lambda_1) + \ln\left(\frac{b}{r}\right)\right]\left(\frac{r}{b}\right) + \frac{p2^{p+1}q^{2p}}{B_1(B_1 - 1)b^{2(^pB_1-1)}}\left(\frac{b}{r}\right)^{B_1-1}. \tag{A11}$$

After some algebraic simplifications, the quasilocal mass $\mathcal{M}$ can be written as

$$\mathcal{M} = \frac{mb}{4} + \frac{m^2 b}{8}\frac{1}{u_1(r)} + \mathcal{O}\left(\frac{1}{u_1(r)}\right)^2, \tag{A12}$$

and by taking limit $r \to \infty$, we obtain

$$M = \frac{mb}{4}. \tag{A13}$$

By summarizing Eqs. (A5), (A9), and (A13), the analogous ADM black hole mass can be written in the general form given by Eq. (3.13).

[1] M. B. Green, J. H. Schwarz, and E. Witten, *Superstring Theory* (Cambridge University Press, Cambridge, United Kingdom, 1987).
[2] G. W. Gibbons and K. Maeda, Nucl. Phys. **B298**, 741 (1988).
[3] M. Dehghani, Phys. Rev. D **96**, 044014 (2017).
[4] M. Dehghani, Phys. Rev. D **99**, 104036 (2019).
[5] J. D. Bekenstein, Phys. Rev. D **5**, 1239 (1972).
[6] C. Teitelboim, Phys. Rev. D **5**, 2941 (1972).
[7] M. Dehghani, Phys. Lett. B **773**, 105 (2017).
[8] S. Fernado and D. Krug, Gen. Relativ. Gravit. **35**, 129 (2003).
[9] H. A. Gonzalez, M. Hassaine, and C. Martinez, Phys. Rev. D **80**, 104008 (2009).
[10] Z. Dayyani, A. Sheykhi, and M. H. Dehghani, Phys. Rev. D **95**, 084004 (2017).
[11] S. W. Hawking, Nature (London) **248**, 30 (1974).
[12] S. W. Hawking, Commun. Math. Phys. **43**, 199 (1975).
[13] S. W. Hawking, Phys. Rev. D **72**, 084013 (2005).
[14] J. D. Bekenstein, Phys. Rev. D **7**, 2333 (1973).
[15] M. Dehghani, Phys. Lett. B **749**, 125 (2015).
[16] J. M. Bardeen, B. Carter, and S. W. Hawking, Commun. Math. Phys. **31**, 161 (1973).
[17] S. W. Hawking, Commun. Math. Phys. **43**, 199 (1975).
[18] S. H. Hendi, S. Panahiyan, B. Eslam Panah, and M. Momennia, Eur. Phys. J. C **75**, 507 (2015).
[19] C. S. Peca and J. P. S. Lemos, Phys. Rev. D **59**, 124007 (1999).
[20] H. W. Braden, J. D. Brown, B. F. Whiting, and J. W. York, Phys. Rev. D **42**, 3376 (1990).
[21] S. H. Hendi, Ann. Phys. (Amsterdam) **333**, 282 (2013).
[22] M. Dehghani, Phys. Rev. D **94**, 104071 (2016).
[23] M. Dehghani and S. F. Hamidi, Phys. Rev. D **96**, 044025 (2017).
[24] E. Witten, Adv. Theor. Math. Phys. **2**, 253 (1998).
[25] E. Witten, Adv. Theor. Math. Phys. **2**, 505 (1998).
[26] J. M. Maldacena, Adv. Theor. Math. Phys. **2**, 231 (1998).
[27] M. Born and L. Infeld, Proc. R. Soc. A **143**, 410 (1934).
[28] M. Born and L. Infeld, Proc. R. Soc. A **144**, 425 (1934).
[29] H. H. Soleng, Phys. Rev. D **52**, 6178 (1995).
[30] A. Sheykhi and A. Kazemi, Phys. Rev. D **90**, 044028 (2014).
[31] M. Dehghani, Phys. Lett. B **793**, 234 (2019).
[32] A. Sheykhi, F. Naeimipour, and S. M. Zebarjad, Phys. Rev. D **91**, 124057 (2015).
[33] S. H. Hendi, Gen. Relativ. Gravit. **48**, 50 (2016).
[34] S. H. Hendi, S. Panahiyan, B. Eslam Panah, and M. Momennia, Eur. Phys. J. C **76**, 150 (2016).
[35] M. Dehghani, Phys. Rev. D **98**, 044008 (2018).
[36] A. Sheykhi, Phys. Rev. D **86**, 024013 (2012).
[37] M. Kord Zangeneh, A. Sheykhi, and M. H. Dehghani, Phys. Rev. D **91**, 044035 (2015).
[38] T. P. Sotiriou and V. Faraoni, Phys. Rev. Lett. **108**, 081103 (2012).
[39] S. H. Mazharimousavi and M. Halilsoy, Mod. Phys. Lett. A **30**, 1550177 (2015).
[40] Y. Ling, C. Niu, J. P. Wu, and Z. Y. Xian, J. High Energy Phys. 11 (2013) 006.
[41] V. Faraoni, Phys. Rev. D **95**, 124013 (2017).
[42] M. Dehghani, Int. J. Mod. Phys. D **27**, 1850073 (2018).
[43] M. Dehghani and S. F. Hamidi, Phys. Rev. D **96**, 104017 (2017).
[44] M. Kord Zangeneh, M. H. Dehghani, and A. Sheykhi, Phys. Rev. D **92**, 104035 (2015).
[45] M. Dehghani, Phys. Lett. B **785**, 274 (2018).
[46] M. M. Stetsko, Phys. Rev. D **99**, 044028 (2019).
[47] M. Dehghani, Phys. Rev. D **99**, 024001 (2019).
[48] M. Dehghani, Phys. Lett. B **777**, 351 (2018).
[49] S. H. Hendi, N. Riazi, S. Panahiyan, and B. Eslam Panah, arXiv:1710.01818.
[50] M. Dehghani, Eur. Phys. J. Plus **133**, 474 (2018).
[51] O. Kichakova, J. Kunz, E. Radu, and Y. Shnir, Phys. Lett. B **747**, 205 (2015).
[52] Y. S Myung, Y-W. Kim, and Y-J. Park, Phys. Rev. D **78**, 084002 (2008).

[53] M. H. Dehghani, A. Sheykhi, and Z. Dayyani, Phys. Rev. D **93**, 024022 (2016).
[54] S. H. Hendi, S. Panahiyan, and M. Momennia, Int. J. Mod. Phys. D **25**, 1650063 (2016).
[55] S. H. Hendi, S. Panahiyan, and B. Eslam Panah, Eur. Phys. J. C **75**, 296 (2015).
[56] S. H. Hendi, B. Eslam Panah, S. Panahiyan, and M. Momennia, Eur. Phys. J. C **77**, 647 (2017).
[57] M. Kord Zangeneh, A. Sheykhi, and M. H. Dehghani, Phys. Rev. D **91**, 044035 (2015).
[58] J. D. Brown and J. W. York, Phys. Rev. D **47**, 1407 (1993).
[59] J. D. Brown, J. Creighton, and R. B. Mann, Phys. Rev. D **50**, 6394 (1994).
[60] K. C. K Chan, J. H. Horne, and R. B. Mann, Nucl. Phys. **B447**, 441 (1995).
[61] S. H. Hendi, A. Sheykhi, S. Panahiyan, and B. Eslam Panah, Phys. Rev. D **92**, 064028 (2015).
[62] S. H. Hendi, M. Faizal, B. Eslam Panah, and S. Panahiyan, Eur. Phys. J. C **76**, 296 (2016).
[63] S. H. Hendi, B. Eslam Panah, S. Panahiyan, and A. Sheykhi, Phys. Lett. B **767**, 214 (2017).
[64] M. Dehghani, Phys. Rev. D **97**, 044030 (2018).
[65] S. W. Hawking and D. N. Page, Commun. Math. Phys. **87**, 577 (1983).
[66] M. Zhang, Gen. Relativ. Gravit. **51**, 13 (2019).
[67] M-S. Ma and R. Zhao, Phys. Lett. B **751**, 278 (2015).